Prace Naukowe Instytutu Maszyn, Napędów i Pomiarów Elektrycznych
Nr 70 Politechniki Wrocławskiej Nr 70

Studia i Materiały Nr 34 2014

induction motor, Direct Torque Control,
Flux-Space-Vector Modulation, field weakening control

Khanh NGUYEN THAC*, Teresa ORLOWSKA-KOWALSKA**

CONTROL OF THE DTC-FSVM BASED INDUCTION MOTOR DRIVE IN A WIDE SPEED RANGE

In this paper the direct flux and torque control structure based on Flux-error Space Vector Modulation (DTC-FSVM) has been analyzed and compared to a classical DTC-SVM system. The control structures have been tested in a wide speed range including field weakening algorithm based on the voltage and current limits of the voltage inverter and the induction motor. The proposed control strategies are verified through simulation with a 3 kW induction motor drive.

1. INTRODUCTION

Induction motors (IM) due to their operational reliability, small size and low cost in comparison to DC motors and permanent magnet synchronous motors, are continuously most popular among the electrical motors applied in the industry [6], [9]. However, the complicated mathematical model of the induction motor entails that complex control methods and structures must be used to obtain the dynamic behavior of these drives similar to classical DC motor drives with cascade control structure. Presently the quite matured control methods, which ensure excellent dynamics of the IM drive, are Field Oriented Control (FOC) and Direct Torque Control (DTC) methods [2]–[4], [6], [9], [13]. Both techniques can be considered as high performance vector controllers based on the decoupling of motor flux and torque. The DTC systems, which were first introduced in the middle of 1980s, ensure a very quick and precise torque control response with relatively simple control structure based on hysteresis controllers for the stator flux and electromagnetic torque [3], [9], [13]. However, classical DTC method has several disadvantages, from which the most

* Department of Electrical and Electronic Engineering, Hanoi University of Mining and Geology, Duc Thang Ward, Bac Tu Liem District, Hanoi, Vietnam, e-mail: nguyenthackhanh@humg.edu.vn

** Institute of Electrical Machines, Drives and Measurements, Wroclaw University of Technology, ul. Smoluchowskiego 19, 50-372 Wroclaw, Poland, e-mail: teresa.orlowska-kowalska@pwr.wroc.pl

important is a variable switching frequency. Nowadays, apart from classical DTC method, based on the voltage switching table (ST-DTC), some new direct torque control techniques have been developed [4]–[6]. The overview of the DTC methods was presented in [6].

Simple structure and very good dynamic behavior are main features of classical ST-DTC based schemes. On contrary, the DTC techniques based on Space-Vector--Modulation ensure constant switching frequency, but the control structure is more complicated and first of all contains PI controllers and requires vector transformation of coordinate systems. In these schemes the reference voltage vector is generated based on the torque and flux errors. This reference voltage vector is next utilized for generating inverter switching states using the principle of SVM (Space Vector Modulation).

Recently a novel approach of the direct flux and torque control with SVM has been proposed [12], which consists in replacing the reference voltage vector by reference stator flux-error vector, which is called Flux-error Space Vector Modulation (F-SVM). The stator flux-error vector is used as a main variable for calculation IGBT switching-on times of the VSI (Voltage Source Inverter).

The effectiveness of this control concept has been tested in this paper in a wide speed range of the IM drive system, especially in the field-weakening (FW) region. In these tests the FW method, which ensures maximum DC bus voltage utilization is used. Taking into account a voltage limit and a current limit of inverter and induction motor in FW region (as in [7], [8]), a control strategy for FW-operation-based DTC-FSVM method with maximum torque capability algorithm is presented. The control scheme utilizes the stator flux components as control variables and decreases the d-component of the stator flux as soon as the voltage corresponding to the maximum torque achievable at a given speed tends to exceed the maximum voltage.

2. PRINCIPLE OF THE FLUX-ERROR SPACE VECTOR MODULATION

The stator flux vector control method relies directly on the Faraday's law. Under space vector theory, this law can be written as, $\mathbf{u}_{ind} = T_N d\boldsymbol{\psi}_s / dt$, i.e. the rate of change of the stator flux vector $\boldsymbol{\psi}_s$ is equal to the induced voltage vector ($\mathbf{u}_{ind}$). If stator winding resistance is negligible, the induced voltage is equal to the applied stator voltage ($\mathbf{u}_s$).

In discrete time domain, this equation can be interpreted as

$$\Delta\boldsymbol{\psi}_s = \mathbf{u}_s T_s / T_N = \mathbf{u}_s \tau_s \,, \tag{1}$$

where, T_s is a sampling time period in [s] and $T_N = 1/\Omega_b$ is the nominal time constant in [s], therefore τ_s is defined as *relative sampling time period* in [p.u.].

A vector displacement $\Delta\boldsymbol{\psi}_s^*$ is based on an error between actual $\boldsymbol{\psi}_{s(k)}$ and predicted $\boldsymbol{\psi}_{s(k+1)}$ stator flux vectors (Fig. 1a) [12]; it can be obtained by applying a voltage vector $\mathbf{u}_s^*$ for a time τ_s (Fig. 1b). In three phase voltage space vector controlled VSI, the stator flux-error vector can be defined as:

$$\Delta\boldsymbol{\psi}_s^* = \mathbf{u}_s^*\tau_s = \left(\mathbf{u}_R\tau_R' + \mathbf{u}_L\tau_L' + \mathbf{u}_0\tau_0'\right), \tag{2}$$

where: $\mathbf{u}_R, \mathbf{u}_L$ are the right and left adjacent active voltage vectors in a given sector; $\mathbf{u}_0$ – the zero voltage vectors; τ_R', τ_L', τ_0' normalized ($\tau' = t/T_N$) switching-on times of the right, left and the zero voltage vectors respectively.

In Fig. 1, the stator flux-error vector can be defined by modulus $\Delta\psi_s^* = \left|\Delta\boldsymbol{\psi}_s^*\right|$ and argument γ_s. In a steady state, with the assumption that stator flux ψ_s and stator frequency are constants, the stator flux-error vector components can be calculated as:

$$\left|\Delta\boldsymbol{\psi}_s^*\right| = \Delta\psi_s^* = 2\left|\boldsymbol{\psi}_s\right|\sin\left(\frac{1}{2}\omega_s\tau_s\right), \tag{3}$$

$$\begin{aligned}\gamma_s &= \left[\pi - \left(\frac{1}{2}\pi - \tfrac{1}{2}\omega_s\tau_s\right) + \varepsilon\right] \\ &= \frac{1}{2}\pi + \frac{1}{2}\omega_s\tau_s + \varepsilon.\end{aligned} \tag{4}$$

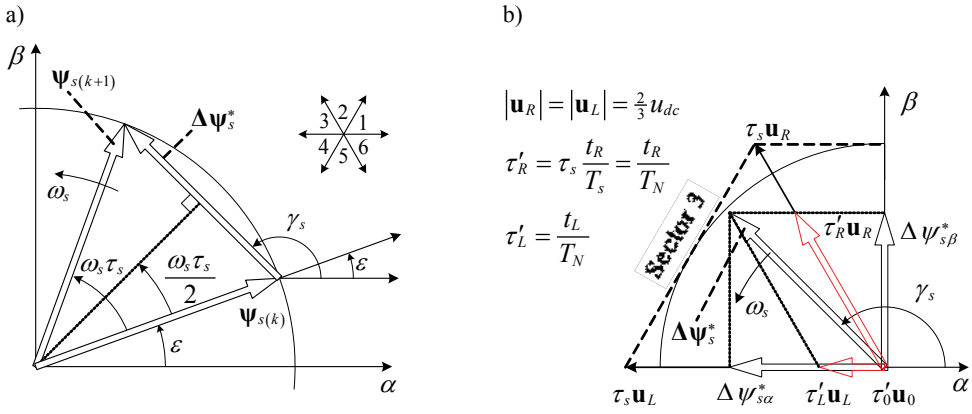

Fig. 1. Trajectory of the stator flux-error vector: a) definition of the stator flux-error vector, b) stator flux-error vector in specific voltage sector

For a small value of the sampling time interval, the product $\omega_s\tau_s$ will be very small. Therefore, $\sin\left(\frac{1}{2}\omega_s\tau_s\right)\approx\frac{1}{2}\omega_s\tau_s$. For example, at angular velocity $\omega_s=1$ [p.u.], if sampling time period T_s is 1 ms, then the difference between actual value $\sin\left(\frac{1}{2}\omega_s\tau_s\right)$ and its approximation $\frac{1}{2}\omega_s\tau_s$ is less than 0.2%. So, the stator flux-error modulus in equation (3) can be simplified as:

$$\Delta\psi_s^*=\omega_s\tau_s\psi_s. \tag{5}$$

Similarly to the well know Voltage Space Vector Modulation (V-SVM) method, with reference stator voltage vector as an input information, in Flux Space Vector Modulation (F-SVM) method the stator flux-error $\boldsymbol{\Delta\psi}_s^*$ can be used as an input information.

In the presented F-SVM, three operation regions are used (like in V-SVM strategy): linear region, overmodulation (divided into region I and region II) and six-step mode. An operation region is defined by modulation index (6):

$$M_i=\frac{\Delta\psi_s^*}{\frac{2}{\pi}\tau_s u_{dc}} \tag{6}$$

where, $\Delta\psi_s^*$ – stator flux-error vector module; u_{dc} – DC link voltage.

Operation regions dependent on modulation index values are shown in the Table 1.

Table 1. Operation regions dependent on modulation indexes

Operation regions			
Linear	Overmodulation		Six-step
	Region I	Region II	
$0\le M_i<0.907$	$0.907\le M_i<0.952$	$0.952\le M_i<1$	$M_i=1$

In the linear operation region, switching-on times can be calculated as follows.

$$t_R=T_s\frac{3}{\pi}\frac{M_i\sin(\pi/3-\alpha)}{\sin(\pi/3)}, \tag{7a}$$

$$t_L=T_s\frac{3}{\pi}\frac{M_i\sin(\alpha)}{\sin(\pi/3)}, \tag{7b}$$

$$t_0=T_s-(t_R+t_L). \tag{7c}$$

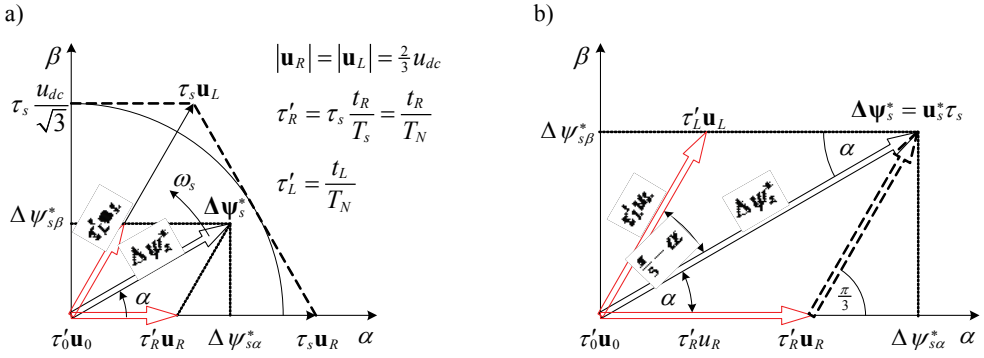

Fig. 2. Flux-error vector modulation in the linear region

In the Fig. 2 an illustration of the Flux-error Vector Modulation in the linear region is given. The overmodulation and six-step operation modes are used in the drive system to enable the full DC link voltage utilization of the converter (details on the overmodulation algorithm was shown in [13]).

3. DIRECT TORQUE CONTROL WITH FLUX-ERROR SPACE VECTOR MODULATION

In the closed-loop flux and torque control methods based on Stator-Flux-Orientation (SFO), the reference stator flux vector is used, therefore its angular frequency, $\omega_{ss} = \omega_m + \omega_r$ (or position angle, $\gamma_{ss} = 1/T_N \int \omega_{ss} dt$) must be known. The mechanical speed, ω_m can be received from the encoder (or well-known speed estimators), so only slip speed must be estimated. There exist different methods for slip speed estimation, which are presented in the references [9], [13]. Thus, the stator flux vector position can be presented as:

$$\gamma_{ss} = \gamma_{ss(k-1)} + \Delta\gamma_{ss}, \tag{8}$$

where: $\gamma_{ss(k-1)}$ – previous angle position in the last sampling time,

$\Delta\gamma_{ss} = \Delta\gamma_{ss}^{\text{stat}} + \Delta\gamma_{ss}^{\text{dyn}}$ – change of the stator flux vector position angle in the current sampling time,

$\Delta\gamma_{ss}^{\text{stat}}$ – stationary change of the stator flux vector position angle,

$\Delta\gamma_{ss}^{\text{dyn}}$ – dynamic change of the stator flux vector position angle.

General stator flux vector movement and its components are illustrated in Fig. 3.

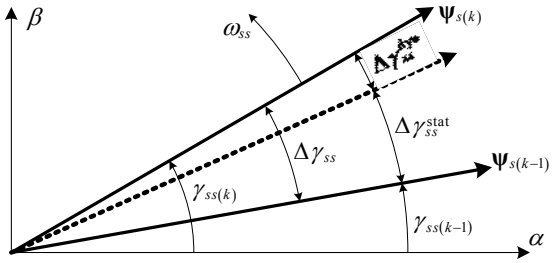

Fig. 3. Stator flux vector position components

The predictive direct stator flux vector control algorithm is proposed in [1], which is equipped with one PID controller. The aim of the controller is to estimate the slip angle, $\Delta\gamma_{slip}$. Another predicted value is a mechanical speed, $\omega_{m\,\mathrm{predic}}$, which multiplied by a sampling time, τ_s, makes mechanical angle, $\Delta\gamma_m$. As a result, change of the stator flux vector angle can be obtained as a sum of the mechanical and slip angles, $\Delta\gamma_{ss} = \Delta\gamma_m + \Delta\gamma_{slip}$ and stator flux vector position (8) can be obtained as:

$$\gamma_{ss}^{*} = \gamma_{ss(k-1)} + \Delta\gamma_m + \Delta\gamma_{slip}\,. \tag{9}$$

Block diagram of this algorithm is shown in Fig. 4.

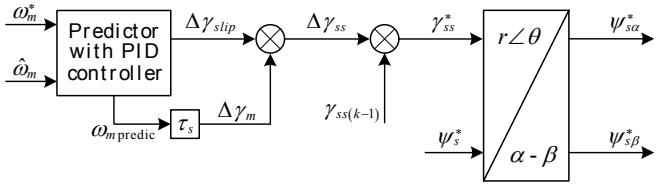

Fig. 4. Prediction of the shifted stator flux vector angle

In the reference [11] authors proved that derivative of the electromagnetic torque is proportional to the instantaneous slip angular frequency, which means we can use a PI controller to control the slip frequency in order to control the electromagnetic torque.

In the case of closed-loop flux and torque control and under constant flux ($\psi_r = \mathrm{const}$), the stator flux vector position angle γ_{ss}^{*} can be calculated as:

$$\gamma_{ss}^{*} = \frac{1}{T_N}\int_0^t \omega_{ss}\,dt = \frac{1}{T_N}\int_0^t \left(\omega_m + \omega_r\right)dt \tag{10}$$

Many schemes used this idea for calculation of the synchronous speed ω_{ss} or stator flux vector position angle γ_{ss} [6, 12] (Fig. 5).

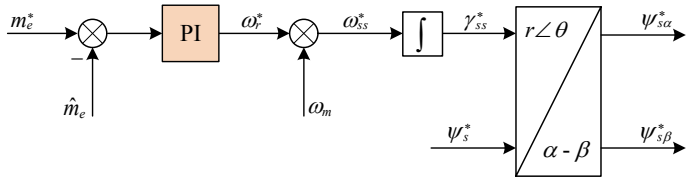

Fig. 5. Slip angular frequency generated by torque controller

Therefore, the flux position angle can be rewritten as:

$$\gamma_{ss}^* = \frac{1}{T_N}\int_0^t \omega_m dt + \frac{1}{T_N}\int_0^t \omega_r^* dt = \gamma_{m(k-1)} + \Delta\gamma_m + \Delta\gamma_{slip} \tag{11}$$

In the steady-state, under discrete time domain, the stationary angle position changes can be calculated as:

$$\Delta\gamma_{ss}^{\text{stat}} = \tau_s \omega_{ss} \,. \tag{12}$$

When the load torque changes, predicted flux vector position angle $\gamma_{ss}^* = 1/T_N \int (\omega_m + \omega_r^*) dt$ deviates from the actual position angle $\gamma_{ss} = 1/T_N \int (\omega_m + \omega_r) dt$, and thus the dynamic angle referred to the torque change is produced $\Delta\delta_\psi = \Delta\gamma_{ss}^{\text{dyn}}$:

$$\Delta\gamma_{ss}^{\text{dyn}} = \gamma_{ss}^* - \gamma_{ss} = \frac{1}{T_N}\int (\omega_r^* - \omega_r) dt \tag{13}$$

Equation (13) shows, that we can obtain the dynamic position angle by a PI controller from difference of the slip angular frequency, $\delta_{\omega r} = \omega_r^* - \omega_r$ [5, 10] (see Fig. 6).

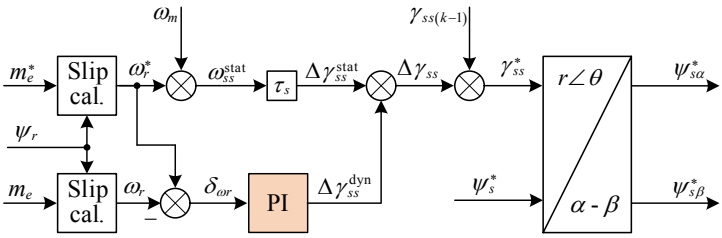

Fig. 6. Dynamic flux vector position generated by slip controller

In the Fig. 6, slip calculation blocks are based on the following expression [9]:

$$\omega_r = \frac{r_r}{\psi_r^2} m_e . \tag{14}$$

To choose the best scheme for stator flux vector position generating, in this section all presented schemes are tested and compared under steady-state and dynamical modes, in a wide speed range. The simulation results for above schemes in high speed region are presented in Fig. 7, for step changes of the load torque (from 0.5s to 0.7s the load torque is reduced 50% from the previous steady state value.)

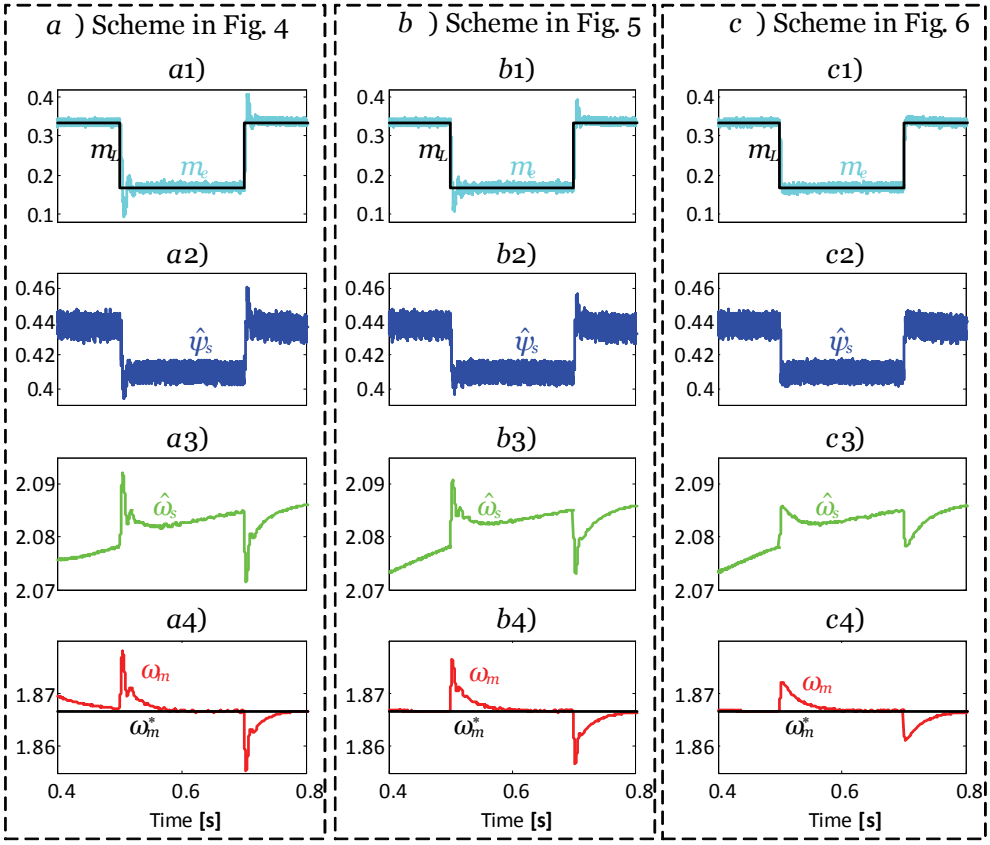

Fig. 7. Simulation results: torque (a1–c1), flux (a2–c2), stator frequency (a3–c3) and speed (a4–c4) transients under load torque changes

These simulation results show that the dynamics of the third scheme (Fig. 6) is very good. As a result, stator flux, electromagnetic torque and speed quickly respond to the reference or load torque changes if compared with other schemes (see Fig. 7c).

According to the above analysis, the block diagram of the DTC-FSVM structure was next tested, presented in Fig. 8. This structure includes the calculation of the stator flux position angle according to the scheme in Fig. 6, due to its best dynamical performance. Additionally the field weakening algorithm with torque limit was used in the chosen DTC-FSVM structure.

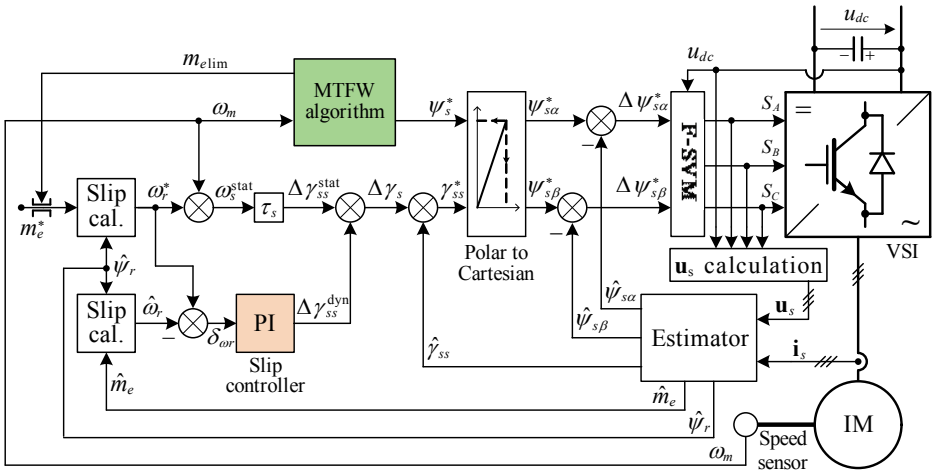

Fig. 8. Chosen DTC-FSVM control of IM drive

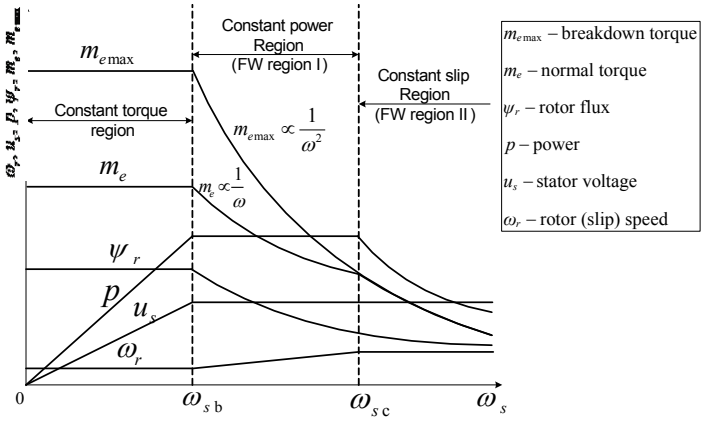

Fig. 9. Control characteristics of the induction motor in constant and weakened flux regions

The operating speed range of the IM drive can be divided in three sub-regions: constant torque region ($\omega_s < \omega_{sb}$), constant power region ($\omega_{sb} \le \omega_s < \omega_{sc}$) and constant slip frequency region ($\omega_s \ge \omega_{sc}$) [6], as is shown in Fig. 9 (where ω_{sb}, ω_{sc} are base and critical stator angular speeds).

In the block scheme of Fig. 9, the Torque-Maximized Field Weakening (TMFW) algorithm described detail in [7], [8] is used. In this algorithm, only mechanical speed (ω_m) and DC link voltage (u_{dc}) are input variables, therefore it is not dependent on the reference frame (RFO or SFO) chosen for its development.

4. TEST RESULTS

In the following figures, simulation results are presented to show the comparison between two DTC structures under the same MTFW algorithm and operation conditions, such as voltage, load torque and reference speed. The test results for the classical DTC-SVM structure (with V-SVM) are plotted in the left hand side of each figure, while the results of the DTC-FSVM scheme are presented in the right hand side, respectively. All tests were performed for 3.0kW, 1400 rpm induction motor and following per-unit parameters: r_s = 0.0707, r_r = 0.0637, x_s = x_r = 1.9761, x_M = 1.8780, ψ_{rN} = 0.8 (calculated according [12]. Simulations were performed for the same voltage and current limit constraints ($u_{\max} = 0.64$ [p.u.], $i_{\max} = 1.5$ [p.u.]), thus the value of the base and critical speeds were obtained as $\omega_{mb} = 0.55$ [p.u.] and $\omega_{mc} = 1.27$ [p.u.].

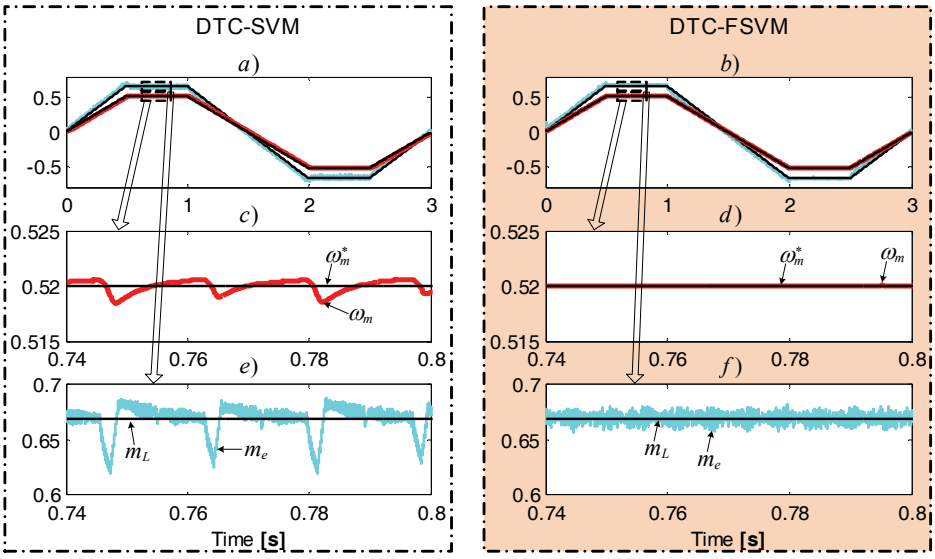

Fig. 10. Simulation results: start up, steady state at ω_m = 0.52 [p.u.] and breaking cycle in both directions: (a, b) reference and motor speed, load and motor torque, (c–f) zoom in the speeds and torques at steady state

In Fig. 10 simulation results under linear speed reference ramp start-up and steady state at $\omega_m^* = 0.52$ [p.u.] speed (constant torque region), for maximum load torque $m_L = m_N$ and breaking cycle in both directions are shown.

In the next Fig. 11 simulation results under linear speed reference ramp start-up and steady state at the speed $\omega_m^* = 1.0$ [p.u.] (FW region I) and breaking cycle in both directions are presented. Maximum load torque satisfies constant power condition, $\omega_m^* m_L = \omega_{mb} m_N$.

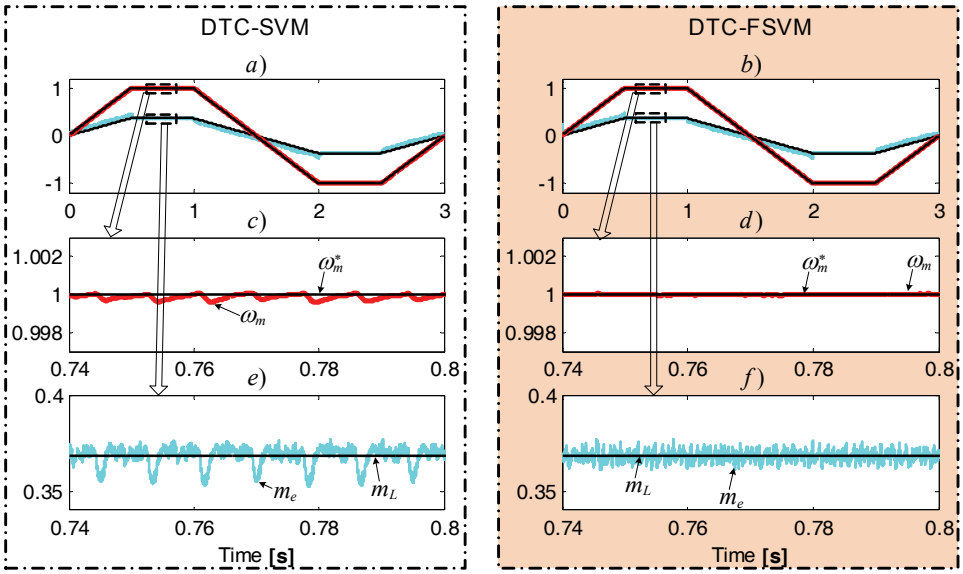

Fig. 11. Simulation results: Start up, steady state at ω_m^* = 1.0 [p.u.] and breaking cycle in both directions: (a, b) reference and motor speed, load and motor torque, (c–f) zoom in the speeds and torques at steady state

It can be seen from Fig. 10 and Fig. 11, that speed and torque transients of the DTC-FSVM scheme are much smoother then for the DTC-SVM scheme.

Next, the simulation results for the FW region II are presented in Fig. 12. In this test, linear speed reference ramp start-up, next steady state operation at the speed $\omega_m^* = 1.8$ [p.u.] and then breaking process, with maximum steady state load torque equal 0.175 [p.u.] were applied for both DTC systems.

Under these operation conditions, the load torque is close to the torque limit (see Fig. 12e, f), therefore the PI controllers are working in nonlinear mode. As a result, both systems will be working in the overmodulation mode. Operation under over-modulation mode and saturation of the PI controllers cause that the DTC-SVM drive

cannot obtain maximum torque generation and reference speed also (see Fig. 12c). In comparison, the DTC-FSVM can work in dynamic mode, so in this test the VSI operates in six-step mode at steady state and system can obtain the desired speed value (see Fig. 12d).

So it is clearly seen that DTC-FSVM control structure with the flux position angle calculated according scheme of Fig. 6 give much better dynamical and static performance in the torque and speed control in the whole speed range, including overmodulation and six-step mode.

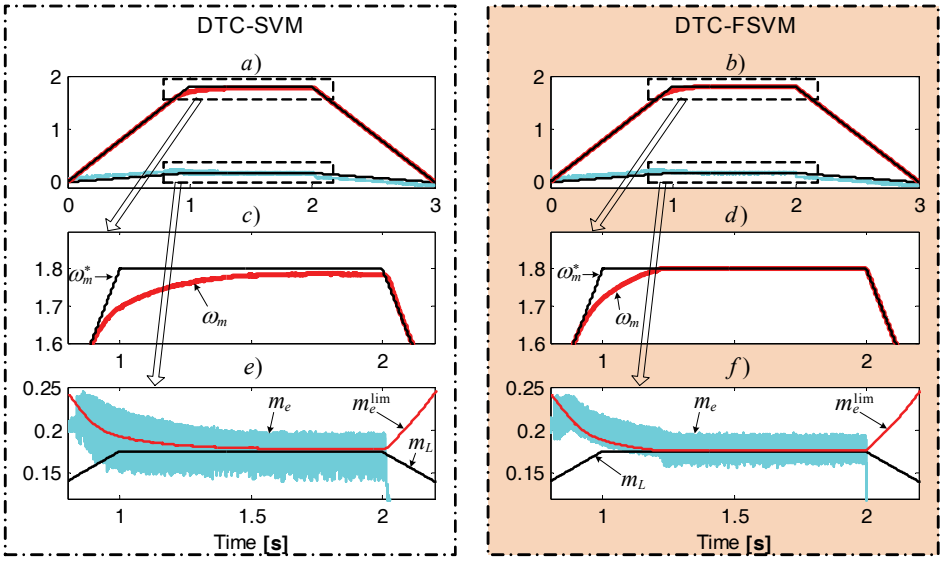

Fig. 12. Simulation results: ramp start up, steady state at ω_m^* =1.8 [p.u.] and braking for two structures: (a, b) reference and motor speed, load and motor torque, (c–f) zoom in the speeds and torques at steady state

6. CONCLUSION

In this paper, the analysis of the flux-error space vector modulation (F-SVM) and three difference concepts of the flux vector position generation in the DTC--FSVM control structure of the induction motor drive are presented. The coordinate transformations, PI torque and flux controllers, which are specific for the classical DTC-SVM (with voltage space vector modulation) are eliminated and only one PI controller for slip speed is used. So, the presented configuration is very simple. In this control structure the torque-maximized flux weakening (TMFW) algorithm can be used and applied for advanced high speed applications

of VSI-fed IM drives, as for spindle and traction application. Test results shown that, the obtained drive systems can operate in a very wide speed range and have excellent torque response as well as smooth transients in the whole range of speed if compared with classical DTC-SVM structure.

REFERENCES

[1] BLAHA P., VACLAVEK P., *A practical realization of PDSFC algorithm using Motorola DSP56F80X*, 2003 IEEE Int. Conf. on Industrial Technol., Maribor, Slovenia, 2003, 554–559.

[2] BLASCHKE F., *The principle of field orientation as applied to the new TRANSVECTOR closed-loop control system for rotating field machines*, Siemens Review, 1972, No. 34, 217–220.

[3] DEPENBROCK M., *Direct self-control of the flux and rotary moment of a rotary-field machine*, 1987.

[4] HABETLER T.G., PROFUMO F., PASTORELLI M., TOLBERT L.M., *Direct Torque Control of Induction Machines Using Space Vector Modulation*, IEEE Trans. on Industry Appl., Sept.–Oct. 1992, Vol. 28, 1045–1051.

[5] HEISING C., STAUDT V., STEIMEL A., *Speed-sensorless stator-flux-oriented control of induction motor drives in traction*, 2010 First Symposium on Sensorless Control for Electrical Drives (SLED), Padova, Italy, 2010, 100–106.

[6] KAZMIERKOWSKI M.P., KRISHNAN R., BLAABJERG F., *Control in power electronics: selected problems*, Academic Press, 2002.

[7] NGUYEN-THAC K., ORLOWSKA-KOWALSKA T., *Comparative analysis of chosen field weakening methods for the Space Vector Modulated - Direct Torque Controlled drive system*, Scientific Papers of the Institute of Electrical Machines, Drives and Metrology of the Wrocław University of Technology, Vol. 31, 2011, 267–280.

[8] NGUYEN-THAC K., ORLOWSKA-KOWALSKA T., TARCHALA G.J., *Influence of the stator winding resistance on the field-weakening operation of the DRFOC induction motor drive*, Bulletin of the Polish Academy of Sciences. Technical Sciences, 2012, Vol. 60, 815–823.

[9] ORLOWSKA-KOWALSKA, T., *Sensorless induction motor drives*, Oficyna Wydawnicza Politechniki Wrocławskiej, Wrocław, Poland, 2003.

[10] SPICHARTZ M., STEIMEL A., STAUDT V., *Stator-flux-oriented control with high torque dynamics in the whole speed range for electric vehicles*, Emobility – Electrical Power Train, 2010, 1–6.

[11] TAKAHASHI I., NOGUCHI T., *A New Quick-Response and High-Efficiency Control Strategy of an Induction Motor*, IEEE Trans. on Industry Applications, 1986, Vol. IA-22, 820–827.

[12] TRIPATHI A., KHAMBADKONE A. M., PANDA S. K., *Stator flux based space-vector modulation and closed loop control of the stator flux vector in overmodulation into six-step mode*, IEEE Trans. on Power Electronics, 2004, Vol. 19, 775–782.

[13] VAS P., *Sensorless vector and direct torque control*, Oxford University Press, 1998.